Modeling the Climatic Response
to Orbital Variations

John Imbrie and John Z. Imbrie

The astronomical theory of the Pleistocene ice ages holds that variations in the earth's orbit influence climate by changing the seasonal and latitudinal distribution of incoming solar radiation (1 - 3). Because these changes can be calculated with great precision for the past several million years, it is possible in principle to test the theory by comparing the record of Pleistocene climate with a predicted pattern of climatic change. As summarized in the first part of this ar-

climate that are continuous, well correlated, and reasonably well fixed in time. As a result, it has been possible to bypass some of the theoretical problems resulting from our imperfect knowledge of the mechanisms of climatic response by testing the astronomical theory in the frequency domain. For example, it is now clear that a significant part of the observed climatic variance over the past 730,000 years is concentrated in narrow frequency bands near cycles of 19,000,

Summary. According to the astronomical theory of climate, variations in the earth's orbit are the fundamental cause of the succession of Pleistocene ice ages. This article summarizes how the theory has evolved since the pioneer studies of James Croll and Milutin Milankovitch, reviews recent evidence that supports the theory, and argues that a major opportunity is at hand to investigate the physical mechanisms by which the climate system responds to orbital forcing. After a survey of the kinds of models that have been applied to this problem, a strategy is suggested for building simple, physically motivated models, and a time-dependent model is developed that simulates the history of planetary glaciation for the past 500,000 years. Ignoring anthropogenic and other possible sources of variation acting at frequencies higher than one cycle per 19,000 years, this model predicts that the long-term cooling trend which began some 6000 years ago will continue for the next 23,000 years.

ticle, early attempts to make such a test encountered both observational and theoretical difficulties. On the one hand, geologists found that their climatic records were discontinuous and difficult to date with sufficient accuracy. On the other hand, climatologists were uncertain how the climate system would respond to changes in the income side of the radiation budget.

During the past 25 years, and particularly over the past decade, the situation has improved dramatically. On the observational side, new techniques for acquiring, interpreting, and dating the paleoclimatic record—particularly as applied to deep-sea piston cores—have yielded many records of late Pleistocene

John Imbrie is Henry L. Doherty professor of oceanography, Brown University, Providence, Rhode Island 02912. John Z. Imbrie is a National Science Foundation predoctoral fellow in the Department of Physics, Harvard University, Cambridge, Massachusetts 02138.

23,000, and 41,000 years—as predicted by the simplest and most general (linear) model of climatic response (4-10). If the response is indeed only linear, then statistical analysis suggests that as much as 25 percent of the observed variance is explained by orbital forcing (11, 12). If the response is significantly nonlinear, then the percentage of explained variance may well be larger (13). In any event, there is substantial empirical evidence both in the frequency domain and in the time domain that orbital influences are actually felt by the climate system.

At the same time, significant advances have been made in climate theory. A new generation of radiation-balance models has recently been applied to the ice-age problem with results that support the astronomical theory (14-17). These theoretical developments, combined with advances in paleoclimatology, indicate that there is an opportunity to

make a fundamental shift in research strategy (17). Specifically, we should aim to identify mechanisms by which different parts of the climate system respond to changes in radiative boundary conditions. The importance of this opportunity is that both the temporal and the spatial structure of these changes can be specified exactly (18, 19). Except for studies of the annual cycle, we know of no other problem in climate dynamics where the primary external forcing terms are known so precisely.

This opportunity can be exploited most effectively by comparing geological observations with predictions derived from physically based models of climate. In the second part of this article we review the available models and distinguish between two types: an *equilibrium model* of the form $y = f(x)$, where the climatic state (y) has come to equilibrium with the fixed orbital boundary condition (x), and a *differential model* of the form $dy/dt = f(y,x)$, where integration yields a history of climatic response to changing boundary conditions.

In the third section of this article, we recommend a strategy for developing differential models that are physically motivated yet simple enough so that their full explanatory powers can be determined by comparing a wide range of model variants with geological observations. Applying this strategy in the fourth section, we develop a differential model of the form $dy/dt = (1/T_i)(x - y)$. Here, the input x is a single function of time representing the orbital forcing, y is a measure of the total volume of land ice, and T_i is a pair of constants at our disposal. The output of this model compares favorably with the geological record of the past 250,000 years. Thus, the model's prediction for the next 100,000 years is useful as a basis for forecasting how climate would evolve at orbital frequencies in the absence of anthropogenic disturbance. For intervals older than about 250,000 years, however, the match between actual and model climates deteriorates with age. In a final section, we compare existing differential models, suggest some improvements that could be incorporated in future models, and discuss the fundamental questions of climatic sensitivity and predictability.

Astronomical Theory of Climate

Orbital control of irradiation. If the solar output is assumed to be constant, the amount of solar radiation striking the top of the atmosphere at any given latitude and season is fixed by three ele-

 943
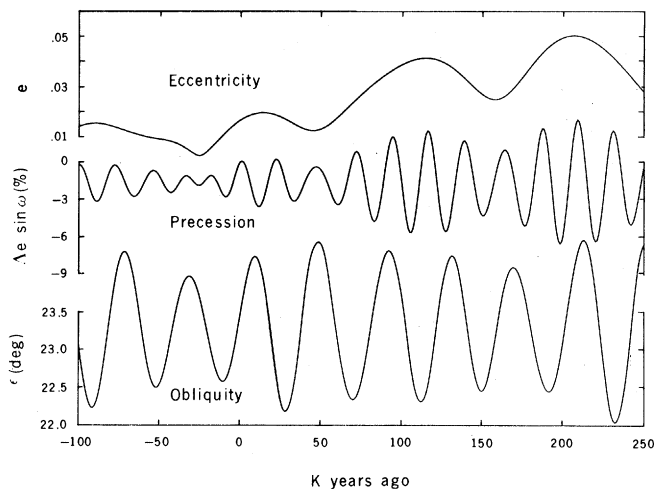
Fig. 1. Variations in orbital geometry as a function of time (K = 1000), according to calculations by Berger (*19*). The climatic effect of precession is recorded as an index ($\Delta e \sin \omega$) that is approximately equal to the deviation from its 1950 value of the earth-sun distance in June, expressed as a fraction of the semimajor axis of the earth's orbit.

ments of the earth's orbit: the eccentricity (*e*), the obliquity of the ecliptic (*ε*), and the longitude of perihelion (*ω*) with respect to the moving vernal point (*19*). Integrated over all latitudes and over an entire year, the energy influx depends only on *e*. However, the geographic and seasonal pattern of irradiation essentially depends only on *ε* and on *e* sin *ω*, a parameter that describes how the precession of the equinoxes affects the seasonal configuration of earth-sun distances (*20*). When the value of *e* sin *ω* for A.D. 1950 is subtracted, the resulting precession index, $\Delta(e \sin \omega)$, is approximately equal to the deviation from the 1950 value of the earth-sun distance in June, expressed as a fraction of the (invariant) semimajor axis of the earth's orbit (*19, 21*).

Orbital variation. Each of these orbital elements is a quasi-periodic function of time (Fig. 1). Although the curves have a large number of sinusoidal components, calculated spectra are dominated by a small number of peaks. The most important term in the series expansion for eccentricity has a period calculated by Berger (*22*) to be 413,000 years. Eight of the next 12 terms range from 95,000 to 136,000 years. In low-resolution spectra, these terms contribute to a peak that is often loosely referred to as the 100,000-year eccentricity cycle. In contrast, the spectrum of obliquity is relatively simple, dominated by components with periods near 41,000 years. The main components of the precession index have periods near 23,000 and 19,000 years. In low-resolution spectra, these are seen as a single peak near 22,000 years.

The geometry of past and future orbits has been calculated several times (*23*); the most recent work is that of Berger (*19*), whose results are used in this article (*24*). The present value of *e* is 0.017. Over the past million years, this value

has ranged from 0.001 to 0.054. Over the same interval, the value of *ε* (now 23.4°) has ranged from 22.0° to 24.5°; and the precession index (defined as zero for A.D. 1950) has ranged from −6.9 to 3.7 percent.

Climatic impact of orbital change. The income side of the earth's annual radiation budget is the solar energy received at the top of the atmosphere each year. By determining how this income is distributed in time and space, the geometry of the orbit controls both the march of the seasons and the latitudinal arrangement of climatic zones. Therefore, any change in the three orbital elements that fix the irradiation pattern must bring about some climatic change. For example, if eccentricity and obliquity were both reduced from their present values to zero, the seasonal cycle would vanish and pole-to-equator contrasts would sharpen. Or if the summer solstice were shifted toward perihelion and away from its present position relatively far from the sun, summers in the Northern Hemisphere would become warmer (and winters colder) than they are today.

Evolution of ideas. In 1864, Croll (*1*) pointed out that orbitally driven variations in the annual energy influx depend only on eccentricity and are on the order of e^2, or 0.1 percent. Like others who have considered the matter since (*14, 19*), he concluded that the direct influence of these variations was probably too small to be detectable. However, he argued that variations in the seasonal influx—which is a joint function of the three orbital elements—were large enough to trigger a substantial climatic response, namely the cycle of Pleistocene ice ages.

By 1930, Milankovitch (*2*) had transformed Croll's semiquantitative argument into the mathematical framework of an astronomical theory of climate. Ap-

plying the laws of radiation to the orbital calculations of Pilgrim (*25*), he drew a set of curves showing how the irradiation intensity during the summer and winter half-years varies as a function of time and latitude over the past 600,000 years. At all latitudes, the calculated range of variation exceeds 5 percent of modern values. Following a suggestion of Köppen and Wegener (*26*), Milankovitch concluded that the intensity of radiation received at high northern latitudes during the summer was critical to the growth and decay of ice sheets (*27*). Accordingly, he focused attention on a curve representing variations in radiation received during the summer half-year at 65°N (*3, 26*). Here, variations exceed 8 percent of modern values (*28*). This particular version of the astronomical theory is often referred to as the Milankovitch theory of the ice ages.

Since the work of Croll and Milankovitch, many investigations (*29*) have been aimed at the central question of the astronomical theory of the ice ages: Do changes in orbital geometry cause changes in climate that are geologically detectable? On the one hand, climatologists have attacked the problem theoretically by adjusting the boundary conditions of energy-balance models, and then observing the magnitude of the calculated response. If these numerical experiments are viewed narrowly as a test of the astronomical theory, they are open to question because the models used contain untested parameterizations of important physical processes. Work with early models suggested that the climatic response to orbital changes was too small to account for the succession of Pleistocene ice ages (*30, 31*). But experiments with a new generation of models (*14-17*) suggest that orbital variations are sufficient to account for major changes in the size of Northern Hemisphere ice sheets.

On the other hand, geologists have proceeded empirically; that is, they have attempted to match the historical record of climate against astronomical predictions. For many years, these investigations met with three difficulties: incompleteness of the stratigraphic record, uncertainties in Pleistocene chronology, and ambiguities stemming from a priori assumptions about response mechanisms. Since 1955, however, these difficulties have been largely resolved (*32, 33*), and a substantial body of evidence has been presented that changes in orbital geometry do cause changes in climate that are geologically detectable. In 1968, Broecker *et al.* (*34, 35*) pointed out that the curve for summertime irradiation at

944

45°N was a much better match to the paleoclimatic records of the past 150,000 years than the curve for 65°N chosen by Milankovitch. [Although subsequent studies in the time domain have confirmed this correlation (21, 36), it should be kept in mind that statistical correlations of this type do not point unambiguously to an underlying physical mechanism (37).] More recently, spectral analysis of climatic records of the past 450,000 (5, 6) and 730,000 (7–10) years has provided substantial evidence (summarized below in the subsection on the response spectrum) that at least near the frequencies of variation in obliquity and precession, a considerable fraction of the climatic variance is driven in some way by insolation changes accompanying changes in the earth's orbit. Moreover, certain phase relations between orbital forcing and climatic response are reasonably well defined. At a frequency of one cycle per 41,000 years, for example, isotopically recorded changes in ice volume lag obliquity by about 9000 years (5, 6).

Current status. This is not to say that all important questions have been answered. In fact, one purpose of this article is to contribute to the solution of one of the remaining major problems: the origin and history of the 100,000-year climatic cycle. At least over the past 600,000 years, almost all climatic records are dominated by variance components in a narrow frequency band centered near a 100,000-year cycle (5–8, 12, 21, 38). Yet a climatic response at these frequencies is not predicted by the Milankovitch version of the astronomical theory—or any other version that involves a linear response (5, 6). This follows from the fact that irradiation spectra are characterized almost completely by frequencies reflecting changes in obliquity ϵ and precession ($e \sin \omega$). Eccentricity controls only the amplitude of the precession effect; its frequency components do not appear in the precession spectrum (39, 40). Because changes in insolation that depend directly on eccentricity are generally considered to be quantitatively insignificant, it would not be reasonable to formulate a model in which the climatic response depends directly on this parameter. Another problem is that most published climatic records that are more than 600,000 years old do not exhibit a strong 100,000-year cycle. For example, it is virtually absent from isotopic records of planetary ice volume that date from earlier parts of the Pleistocene Epoch (41), although it is probably an important component of soil records from Central Europe that span the past 2

million years (42). As more detailed studies of older marine sequences become available, it will be interesting to see if the 100,000-year cycle is really absent from this climatic record.

Strategy shift. Whatever the outcome of future research on the 100,000-year problem may be—and whatever stochastic (43, 44) or deterministic (45) processes may operate in addition to the astronomical causes—the conclusion seems inescapable that for at least the past 730,000 years, the climate system has responded to orbital forcing at the frequencies of variation in obliquity and precession. Therefore, we argue that the time has come to make a fundamental shift in research strategy: instead of using numerical models of climate to test the astronomical theory, we should use the geological record as a criterion against which to judge the performance of physically motivated models of climate (14, 17). Before proceeding further, it is desirable to review the kinds of models that are available (46–52).
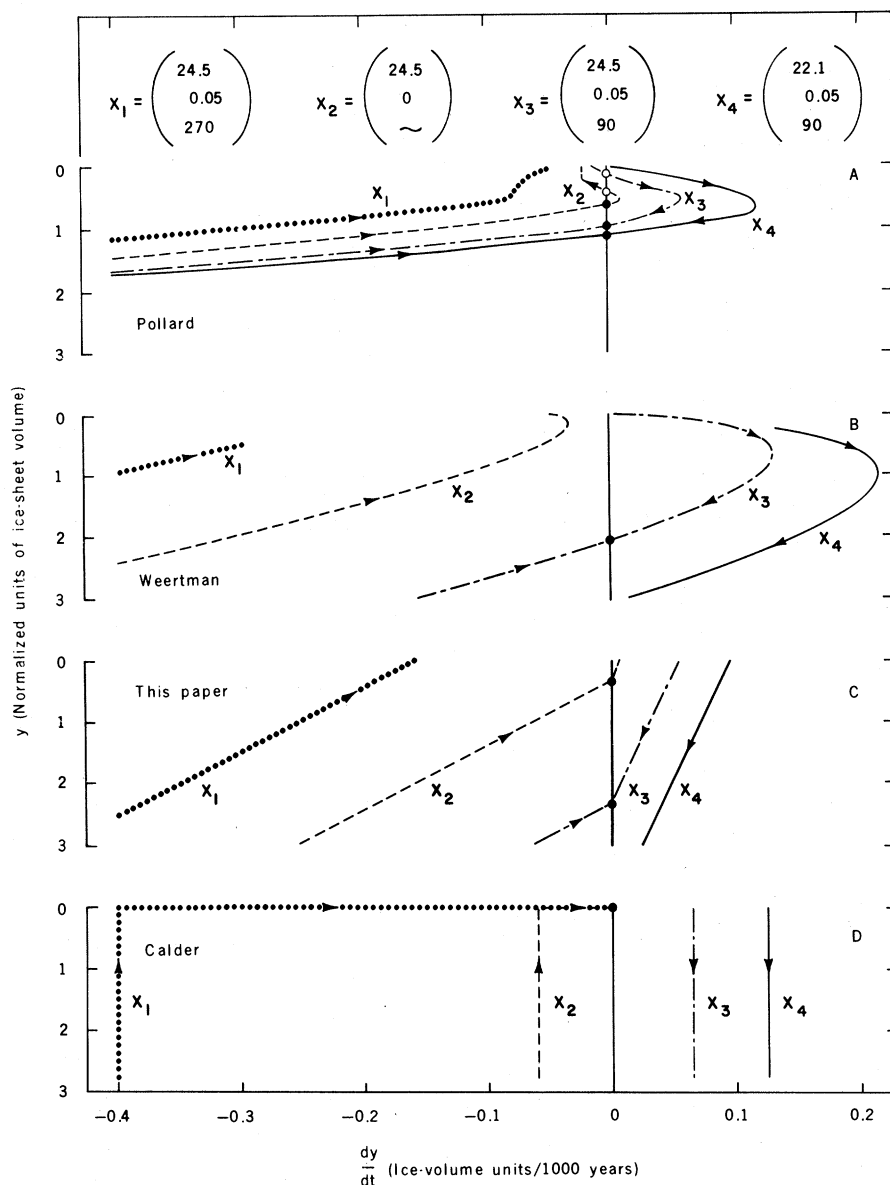

Fig. 2. System functions of four climate models. Each panel is a stability diagram—that is, a plot showing how the rate of change in ice volume (dy/dt) depends on ice-sheet size (y) at various combinations (x_i) of orbital obliquity, eccentricity, and longitude of perihelion. The combination most favoring ice-sheet growth, x_4, has $\epsilon = 22.1°$, $e = 0.05$, and $\omega = 90°$ (perihelion in December). For given values of x, the system either tends to a stable equilibrium (●) or remains in unstable equilibrium (○). If a curve terminates on the axis of zero ice in such a way that for small values of y the curve lies to the left of the $dy/dt = 0$ axis, then zero ice is also a stable fixed point. (A) Stability diagram for Pollard's model (16), taken from his original curves but with the scales transformed to match (B) to (D). (B) Stability diagram for Weertman's model (15). In the neighborhood of zero ice, the curves have a different character and are not shown. (C) Stability diagram for our optimum nonlinear model. The lines continue above the axis of zero ice. (D) Stability diagram for Calder's model (59).

Survey of Response Models

Equilibrium models. Much of the theoretical work done to date has been with equilibrium models of the form $y = f(x)$, where a system function (f) relates the equilibrium climatic state (y) with the orbital boundary condition (x). In some models, the output (y) is a vector quantity representing the climatic response at different sites or in different parts of the system, and the orbital input is specified as a vector $x = x(e, \epsilon, \omega)$.

Two classes of system functions have been used. The first involves setting the output equal to a linear combination of insolation curves. This approach has been widely used by geologists searching for correlations between geological and astronomical time series (*53, 54*). In more complex models, f is generated from a system of differential equations designed to capture the fast physics of the response process. The response $f(x)$ is obtained by integrating the equations to equilibrium at fixed values of x. Several investigators have used models of this type (*14, 17, 30, 31*). In the model developed by Suarez and Held (*14*), the response is forced by seasonal variations in incident radiation at all latitudes. The system function includes albedo feedback and heat storage in an isothermal ocean 40 meters deep. Although the model lacks an ice sheet, the output is a set of latitudes representing the season-

Table 1. Complexity of some differential models.

Model	Number of adjustable parameters (*75*)		
	Input (c_i)	System function (c_f)	Complexity index (c)
This article			
Linear model	2	1	3
Nonlinear model	2	2	4
Calder (*59*)	2	2	4
Weertman (*15*)	3	5	8
Pollard (*16*)	0	12	12

al limits of snow cover and sea ice. The model was run at 5000-year intervals over the past 150,000 years, with successes as well as failures that are typical of equilibrium models. During a model ice age, the latitude of the Northern Hemisphere snow limit shifts southward by a realistic 20°. However, as would be expected with an equilibrium model, the geological record of climate lags significantly behind the model's response.

Differential models. To understand the time-dependent behavior of the system, including the observed lags between orbital forcing and the climatic response, a differential model of the form $dy/dt = f(x,y)$ is required (*55*). As before, f represents the system function, x is the orbital input, and y is some mea-

sure of the climatic state. Such a model is necessary because the characteristic time scales of the growth and decay of ice sheets are known to be of the same order of magnitude as the time scales of orbital forcing (*56, 57*).

In a pioneering study of this kind, Weertman (*15*) modeled the fluctuations of a continental ice sheet as a function of changing solar radiation. The profile of this model ice sheet is governed by the assumptions that ice flows as a perfectly plastic solid and that the crust subsides isostatically. Input to the model is the radiation received at 50°N during the summer half-year; output is the extent of the ice sheet (in kilometers). The system function is a set of equations containing five parameters, each of which may be adjusted within physically reasonable limits. A typical system function is shown in Fig. 2B. Experiments designed to simulate the glacial response to orbital variations over the past 2 million years indicate that the model physics is adequate to account for the magnitude of the known fluctuations in ice-sheet dimensions. The structure of the model response in the time domain is quite sensitive to small adjustments in certain parameters, although the response of the model in the frequency domain is more robust (*58*). In addition to significant responses at the forcing periods (near 19,000, 23,000, and 41,000 years), spectra calculated from the model output
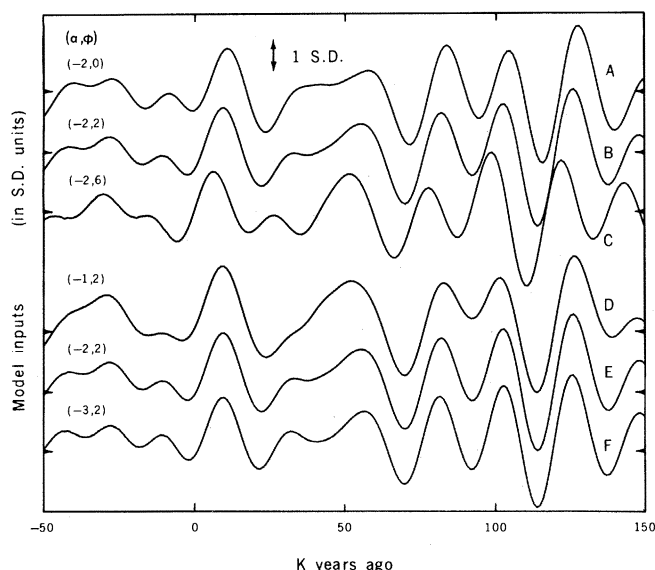

Fig. 3 (left). Family of orbital curves representing the range of model inputs explored in this article. Each curve is a function $x = \epsilon + \alpha e \sin(\omega - \phi)$, where the orbital elements ϵ, e, and ω are functions of time and α and ϕ are adjustable parameters. Each curve corresponds in shape to some irradiation curve. For example, curve B corresponds to the irradiation curve for July at 65°N (*37*). Curves have been normalized to have zero mean (indicated by marks) and unit standard deviation. Values of ϕ are given in thousands of years, with the convention that $2\pi = 22,000$ years.   Fig. 4 (right). Response characteristics of the system function of our optimum model. This function has a mean time constant $T_m = 17,000$ years, and a ratio of 4 : 1 between the time constants of glacial growth and melting. (A) System response to a step input. (B) System response to an orbital input ($\alpha = -2$ and $\phi = 2000$ years) corresponding to an irradiation curve for July at 65°N. As in Fig. 3, the input curve is normalized to zero mean and unit standard deviation. The response curve is not normalized here as it is in Figs. 5 to 8.
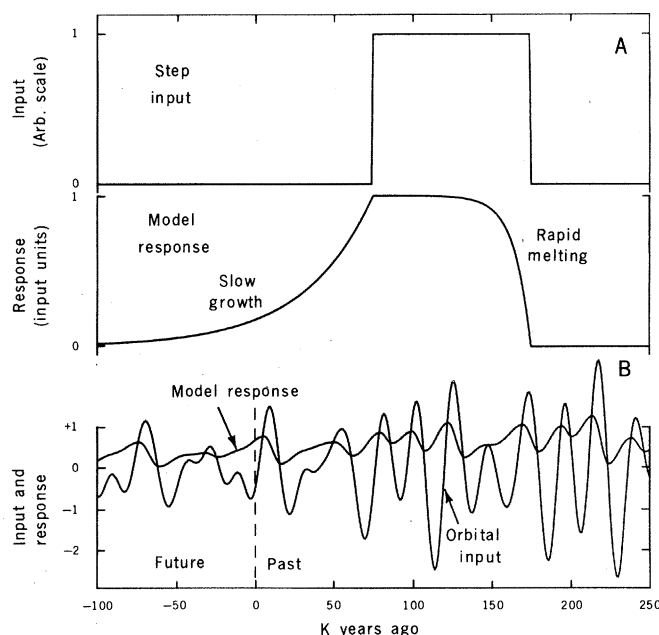
exhibit significant long-period responses in the range 100,000 to 400,000 years—responses which Birchfield and Weertman (58) attribute to nonlinearities associated with the growth and decay of ice sheets.

A considerable advance in modeling complexity was recently made by Pollard (16), who coupled Weertman's ice-sheet model to an energy-balance model of the atmosphere. The model extends over 180° of latitude, is averaged over 360° of longitude, and has two polar ice caps. The weather during any given year is a joint function of the incoming radiation and the extent of the ice sheets. Model input is the radiation received each month at all latitudes; output is the latitude of the equatorward tip of the Northern Hemisphere ice sheet. The system function is a set of equations with 12 adjustable parameters to describe energy transfers and ice-sheet dynamics (Fig. 2A). As in Weertman's model, simulation experiments covering the last 300,000 years reveal substantial sensitivity to parameterization. One choice of parameters gives a reasonably accurate simulation of the climate record of the past 150,000 years, but the earlier record is not well simulated.

A much simpler differential model was proposed by Calder (59). Here, the input is the radiation received at 50°N during the summer half-year, and the output is an estimate of global ice volume. The system function is derived by fixing the values of two parameters (a critical value of the input, and a ratio of response rates above and below this value) and by imposing an upper limit on the output (Fig. 2D). According to experiments we have performed, the output is quite sensitive to small changes in the values of these parameters. For one choice of parameters, Calder gives a simulation extending over the past 800,000 years. The results for the past 150,000 years are quite good. As documented below, the spectrum of this output contains significant power at cycles of 100,000 years and longer.

Developing Differential Models

Development strategy. We wish to formulate a strategy that takes advantage of our knowledge of the history of climate's response to changes in the irradiation pattern. As a starting point, we choose to model global ice volume because there is a continuous isotopic record of this quantity over the past million years (7, 33), and because the cryosphere is probably the only part of the climate system whose characteristic time scales of response are of the same order as the time scales of the orbital forcing (57). If the history of the ice sheets could be successfully simulated, the extent of the ice sheets and the configuration of the earth's orbit could be used as boundary conditions for modeling the faster responses of the atmosphere and the ocean.

One possible strategy for understanding the behavior of the Pleistocene ice sheets is to apply all available knowledge of climate physics to the creation of the most realistic model possible. As described above, Pollard and Weertman have made considerable progress in this direction—yet results fall short of an adequate simulation. In the remainder of this article, we will follow an alternative strategy which attempts to capture the essential features of more complex models in a class of simple models. Perhaps the chief virtue of this strategy is that it becomes possible to uncover the full explanatory power of a given class of models by tuning—that is, by adjusting the model parameters over a range of physically reasonable values until the optimum model variant is identified. If the optimum model is unable to predict important features of the paleoclimatic record, then its failures can be used to suggest improvements in the basic structure
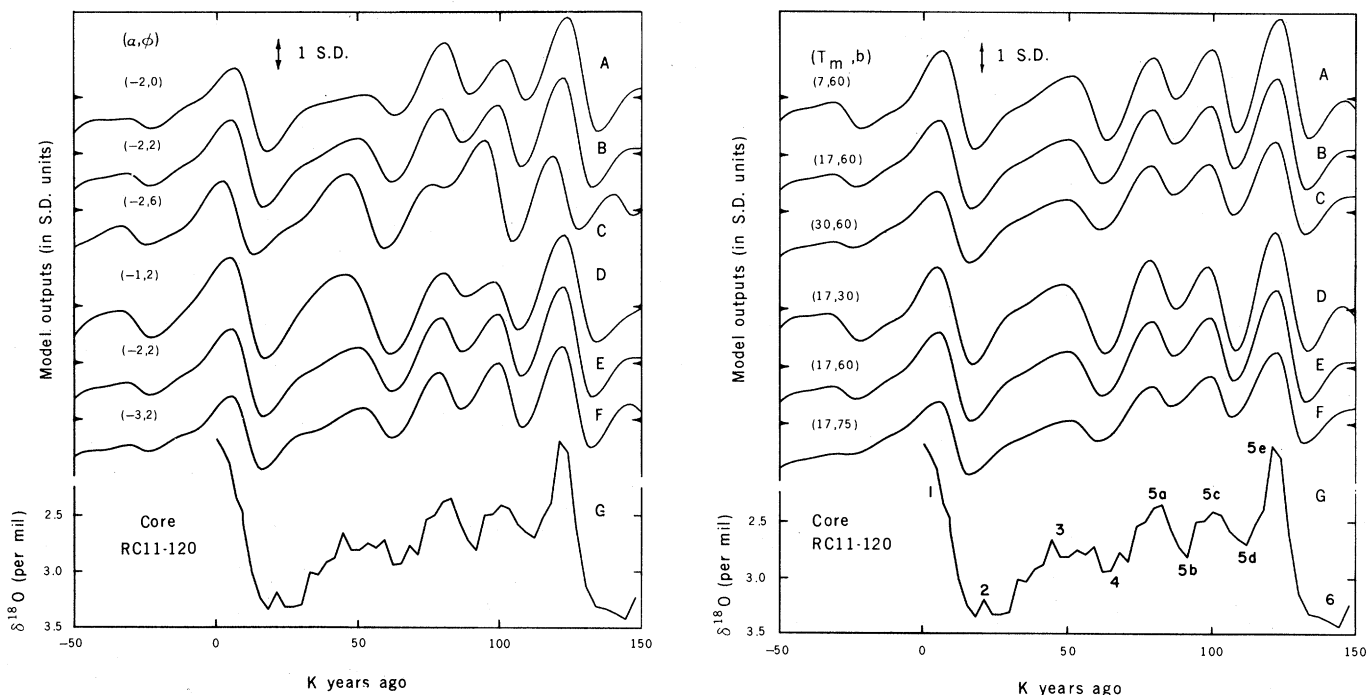

Fig. 5 (left). Family of model output curves illustrating how variations in orbital input affect the output of a given system function. Each of the input curves (Fig. 3) has been processed through the system function of the optimum model (T_m = 17,000 years, b = 0.6). Model outputs (curves A to F) may be compared with isotopic data (5) on climate (curve G). The scale for curves A to F is as in Fig. 3; $\delta^{18}O$ is the per mil enrichment of oxygen-18.   Fig. 6 (right). Family of model output curves illustrating how variations in the system function affect the output when the orbital input curve is fixed. The input (curves B and E in Figs. 3 and 5) is defined by α = −2 and ϕ = 2000 years. Each system function is defined by a mean time constant T_m (in thousands of years) and a nonlinearity coefficient b (expressed in percent). Model outputs (curves A to F) may be compared with oxygen isotope curve G for core RC11-120 (5), on which the numbered stages of the standard stratigraphy (79) are indicated. The scale for curves A to G is as in Fig. 3.

of the model. At each stage in the development process, knowledge of more complex models should provide useful ideas about what new features ought to be incorporated into the model.

Another reason for developing simple models is that even if a complex model yields a successful simulation, it may be difficult to understand what features of the model are the basis of its success. To achieve this understanding, it would be necessary to simplify the model without destroying its predictive abilities (60). We propose to simplify at the outset.

Model complexity. Tuning a model to the climatic record is an essential feature of our strategy for developing a simple class of differential models. To see how drastically complexity affects one's ability to tune a model, define the complexity (c) to be the total number of adjustable parameters. We include in this total any parameter that can be adjusted within the constraints of physical plausibility to make significant changes in the system function. Some of these parameters may vary over a large range and make large changes in the system function, while others may be relatively restricted. For purposes of comparison, however, we count all of them equally. Some of the parameters (c_f) will occur in the system function. As explained in the next section, others (c_i) will occur in the input, so that $c = c_f + c_i$. In the models previously discussed, c ranges from 4 to 12 (Table 1). If each parameter is adjusted over only three levels, then 3^c experiments are necessary. Such a search procedure for Calder's model (81 experiments) is relatively easy, but for Pollard's it would require more than 500,000 experiments.

Parameterizing the input. At higher levels in the modeling hierarchy, where responses to incoming radiation are calculated for all latitudes and months, the orbital input $x = x(e,\epsilon,\omega)$ has no adjustable parameters. At lower levels, linear combinations of irradiation curves at various latitudes and seasons are the most natural choices for input. How many parameters are required to scan all possible inputs of this form? If the scale of the input makes a difference to a model (as it does for Weertman's), three parameters are required because, to an excellent approximation, any insolation curve is a linear combination of ϵ, $e \sin \omega$, and $e \cos \omega$ (61). However, if only the shape of the input curve is important and the scale is arbitrary, then the number of parameters is reduced to two.

To take advantage of this fact, the input to our model is defined as a single function of time $x = \epsilon + \alpha e \sin (\omega - \phi)$, where α and ϕ are adjustable parameters and ϵ, e, and ω are the orbital elements previously defined (normalized to unit variance). The parameter ϕ controls the phase of the precession effect, and is therefore linked to the season of the insolation curve that x would represent (20). To facilitate comparison with the geological record, we have chosen to define ϕ with respect to the number of years in an average precessional cycle, so that 2π radians equals 22,000 years. The parameter α controls the ratio of precession and obliquity effects, and is therefore related to the latitude of the insolation curve that x would represent. The effect on the input curves of exploring the two-parameter space is shown in Fig. 3.

The system function. In accordance with our general strategy for developing differential models, one should keep both physical principles and the climatic

Table 2. Radiometric estimates for the age of climatic events compared with model estimates. Ages are given in thousands of years before present. Events with radiometric ages were used in tuning our model. Uncertainty limits for radiometric ages include analytical and other sources of error.

| Climatic event	Radiometric age ($\times 10^3$ years)	Reference	Model age ($\times 10^3$ years)
Holocene thermal maximum (near the sites of Northern Hemisphere ice sheets)	6 ± 1	(76)	6
Last glacial maximum (stage 2)	18 ± 2	(77)	17
Ice maximum of stage 4			62
Ice minimum of stage 5a	82 ± 6	(78)	80
Ice maximum of stage 5b			88
Ice minimum of stage 5c	105 ± 6	(78)	100
Ice maximum of stage 5d			107
Ice minimum of stage 5e	125 ± 6	(78)	122
Stage 5-6 boundary (termination II)	127 ± 6	(21)	127
Ice maximum of stage 6			133
Stage 7-8 boundary			243
Stage 9-10 boundary (termination IV)			335
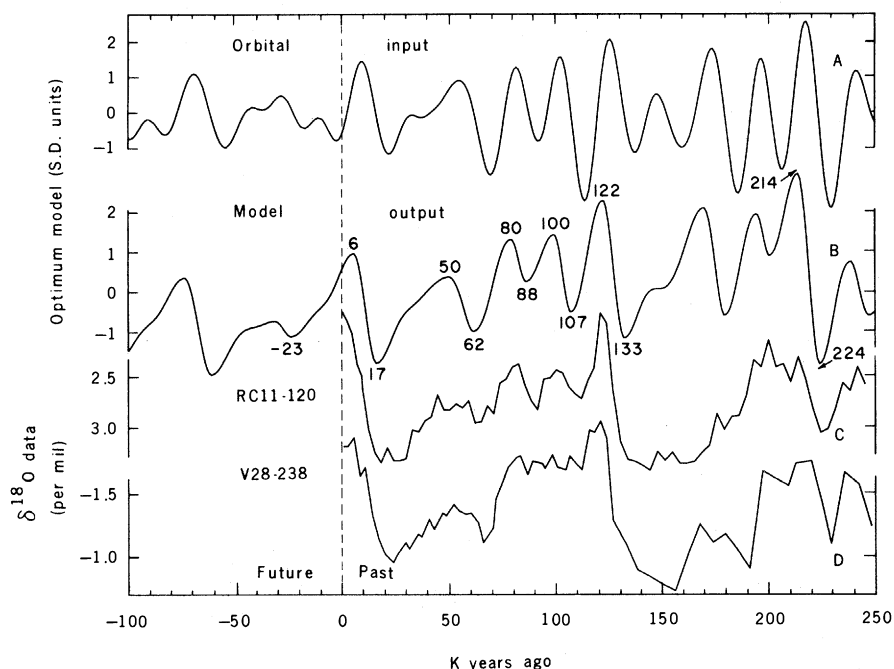
Fig. 7. Input and output of our response model compared with isotopic data on climate of the past 250,000 years. (A) Orbital input (defined by $\alpha = -2$ and $\phi = 2000$ years) corresponding to an irradiation curve for July at 65°N (37). (B) Output of a system function with a mean time constant of 17,000 years and a ratio of 4 : 1 between the time constants of glacial growth and melting. Ages of selected maxima and minima are given in thousands of years. According to this model, the influence of orbital variations over the next 23,000 years will be to enlarge continental ice sheets. (C) Oxygen isotope curve for deep-sea core RC11-120 from the southern Indian Ocean (5). (D) Oxygen isotope curve for deep-sea core V28-238 (7) from the Pacific Ocean [Pee Dee belemnite (PDB) standard]. Curves C and D are plotted against the TUNE-UP time scale of Hays *et al.* (5).

record in mind when designing a class of system functions. In addition, a minimum of complexity is desirable to allow for the tuning process, and the functions should have the potential for producing output spectra close to the known climatic spectra.

A good forum for designing and comparing system functions is the stability diagram (Fig. 2), first introduced in the present context by Pollard (16). The stability diagram is a plot of $dy/dt = f(x,y)$ against y at several fixed values of x. At constant x, points where the curves cross the $dy/dt = 0$ axis are either stable or unstable fixed points of the system, depending on the direction of crossing. The plot is useful in visualizing the behavior of a given system in response to orbital forcing. Thus it can also be used to construct functions that realize a mechanism under consideration.

A Simple Nonlinear Model

Designing the system function. As an application of the ideas presented in the last section, we begin by constructing the simplest model capable of simulating the geologically observed lag between orbital variation and climatic response. Consider the radiation-climate system as a pot of water over a fire, with the heat input varying over time. If the input were constant, the water would approach an equilibrium temperature with some characteristic time constant, T. In a first approximation, the system is linear; that is, the rate of approach toward equilibrium is proportional to the difference between the momentary and equilibrium temperatures. Such a system would be described by the equation

$$\frac{dy}{dt} = \frac{1}{T}(x - y) \qquad (1)$$

A time lag of 9000 ± 3000 years has been measured between the orbital input and the 41,000-year component of the isotopic response (5). By solving Eq. 1 for a sinusoidal input with a period equal to that of the obliquity cycle (41,000 years), we calculate that the time constant needed to produce such a lag would be greater than 8500 years, in rough agreement with time constants derived from physical models of ice sheets (57).

To test this linear model against the geologic record, we used a wide selection of orbital inputs, a range of T between 3000 and 30,000 years, and a mean value of x as an initial value for y. Integration was carried out numerically at time steps of 1000 years starting 1 million years ago, thus allowing the effects of the
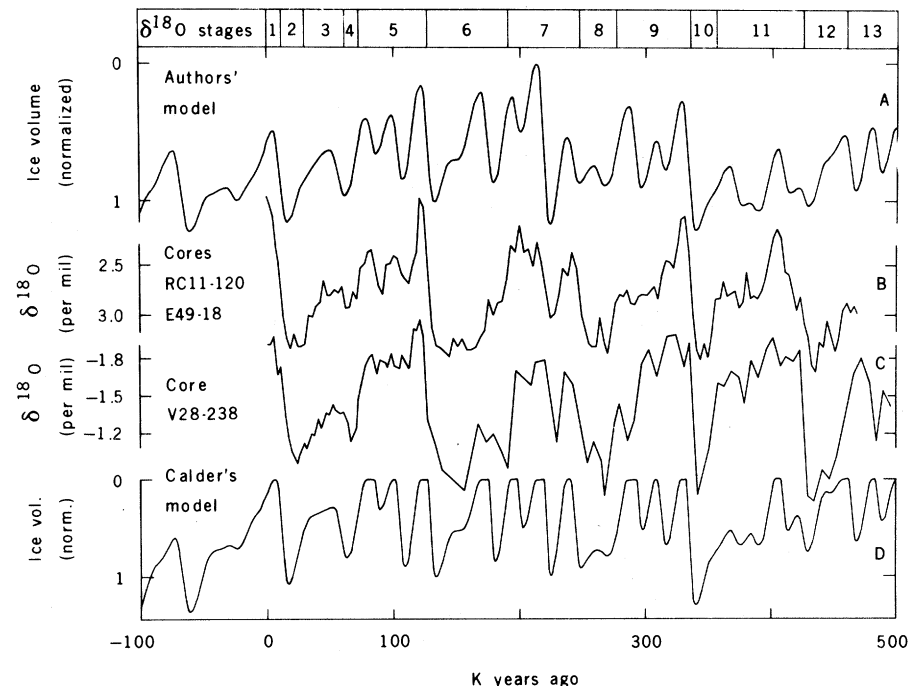
Fig. 8. Two models of climatic response to orbital variation compared with isotopic data on climate of the past 500,000 years. (A) Output of our optimum model described in Fig. 4. (B) Oxygen isotope curve for deep-sea cores RC11-120 and E49-18 from the southern Indian Ocean (5). (C) Oxygen isotope curve for deep-sea core V28-238 (6) from the Pacific Ocean (PDB standard). Curves B and C are plotted against the TUNE-UP time scale of Hays *et al.* (5). (D) Output of a model due to Calder (59). Ice-volume scales in (A) and (D) match those in Fig. 2C and D.

initial condition to die out before reaching the interval studied (the past 500,000 and next 100,000 years). The resulting simulation of the real isotopic curve was poor. Moreover, because the model is linear, the spectrum of the output contained power only at the forcing periods (near 19,000, 23,000, and 41,000 years). None was present at the longer periods associated with eccentricity.

To extract eccentricity frequencies from any model in a physically reasonable way, some form of nonlinearity is required. There are several indications that one source of nonlinear behavior is the tendency for ice sheets to shrink faster than they grow. On the one hand, theoretical arguments suggest that growth times of land-based ice sheets are considerably longer than shrinkage times (62), and that instabilities in marine-based ice sheets probably augment this dynamic asymmetry (63). On the other hand, there is abundant historical evidence from studies of isotopic curves (21) that major glaciations terminate faster than they begin (64). These physical considerations lead us to a simple, nonlinear model of the form $dy/dt = (1/T_i)(x - y)$, where the rate of climatic change is now made inversely proportional to a time constant that assumes one of two specified values depending on whether the climate is warming (T_w) or

cooling (T_c). As with the linear model, if x is held fixed, the output y approaches equilibrium response at $y = x$. The way in which such a model responds to a step input is shown in Fig. 4.

In testing this model we found it convenient to rewrite the system equation as

$$\frac{dy}{dt} = \begin{cases} \dfrac{1+b}{T_m}(x-y) & \text{if } x \geq y \\[2mm] \dfrac{1-b}{T_m}(x-y) & \text{if } x \leq y \end{cases} \qquad (2)$$

where T_m is the mean time constant of the system, and b is a nonlinearity coefficient ($0 \leq b \leq 1$) defined in such a way that larger values of b correspond to larger values of T_c/T_w. Thus, if $b = 0$, Eq. 2 reduces to Eq. 1. As b varies between 1/3 and 2/3, the ratio of time constants varies between 2 and 5.

Tuning: The past 150,000 years. The model's four adjustable parameters are the mean time constant (T_m), the nonlinearity coefficient (b), and two parameters that fix the latitudinal (α) and seasonal (ϕ) characteristics of the orbital input. We first explored this four-parameter space with a reasonably coarse mesh, and found by making rough comparisons of the output against the geological record of the last 500,000 years that the optimum model would lie in the following region: T_m from 7000 to 30,000 years, b

from 0.3 to 0.75, α from -1 to -3, and ϕ from 0 to 6000 years.

Because the chronology and form of the younger climatic record are better known than those of older intervals, and because we wished to allow for the possibility that climate is a nonstationary system, we elected to fine-tune the model against certain features of the geological record of the past 150,000 years. We found that the general form of the model's response was rather robust against the parametric adjustments performed in tuning the model (Figs. 5 and 6). The timing and relative magnitude of the six climatic events for which radiometric ages are given in Table 2 were compared visually with model outputs. These tuning experiments indicate that the optimum model lies in the neighborhood of the following values: $T_m = 17,000$ years, $b = 0.6$ (corresponding to $T_c = 42,500$ years, $T_w = 10,600$ years, and $T_c/T_w = 4$), $\alpha = -2$, and $\phi = 2000$ years (65). The corresponding system function is shown in Fig. 2C. Expressed in terms of radiation for a single month, the orbital input to our optimum model corresponds to the curve for July at 65°N. The same input could also be expressed as combinations of other latitudes and seasons. For example, the insolation for the summer half-year centered on July at 50°N is very close to our input curve.

This simple model's simulation of the past 150,000 years of climate is reasonably good (Table 2 and Fig. 6)—in fact, somewhat better than that achieved by the more complex but untuned models discussed previously. Not only are the calculated ages for the main features of the isotopic curve reproduced rather closely, but also the relative magnitudes of all of the major features of the climate curve are reproduced satisfactorily back through isotopic stage 6. Figure 4 shows that the absolute magnitude of the model's cooling responses would be very large if the input were fixed at a typical
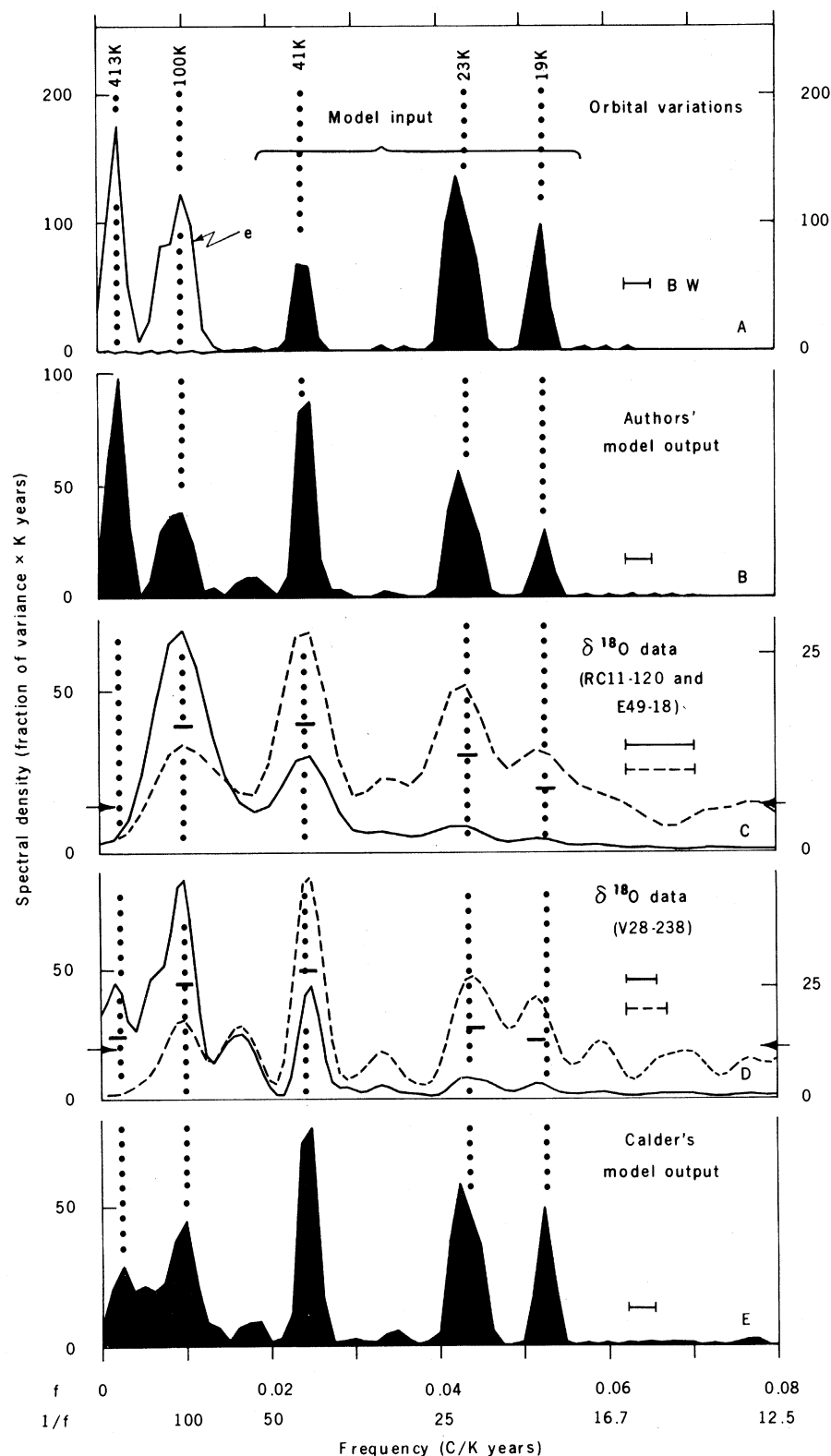

Fig. 9. Spectral density as a function of frequency f (cycles per 1000 years). Climatic spectra are compared with input spectra and output spectra of two climate-response models (80). (A) Solid peaks are the spectrum of the input to our optimum model. Open peaks are the spectrum of variations in eccentricity calculated from data of Berger (19). The dominant periods of these orbital variations, calculated by Berger (22), are indicated in thousands of years and by dotted vertical lines. (B) Spectrum of the output of our optimum model. Note the low-frequency peaks not found in the model input. (C) Solid line shows spectrum of variations in $\delta^{18}O$ from a 468,000-year record in the southern Indian Ocean. Dashed line shows spectrum of same data after prewhitening with a first-difference filter to emphasize details in the higher frequencies. Data are from Hays *et al.* (5), with the spectrum calculated on their TUNE-UP time scale. (D) Solid line shows spectrum of variations in $\delta^{18}O$ from a 730,000-year core record in the Pacific Ocean. Dashed line shows spectrum of the same data after prewhitening with a first-difference filter to emphasize details in the higher frequencies. Isotopic data are from Shackleton and Opdyke (7). Time scale and unprewhitened spectrum are from Kominz *et al.* (8, 9). (E) Spectrum of the output of a response model due to Calder (59). Note the low-frequency peaks not found in this model's orbital input, whose spectrum is almost identical to that shown by solid peaks in (A). Data for (A), (B), and (E) span approximately the last million years. The bandwidth (*BW*) of each spectrum is indicated by horizontal lines. Horizontal bars within peaks in (C) and (D) are the lower bounds of one-sided 90 percent confidence intervals attached to estimates of peak heights. For each prewhitened spectrum in (C) and (D), the level of a red-noise continuum is marked by arrows.

low value. Such extreme responses do not occur in model outputs because the input oscillates relatively rapidly.

Model predictions. Radiometric ages for six of the climatic events listed in Table 2 were used in tuning the model. Calculated ages for the six other events may therefore be considered as predictions to be checked against the results of independent research. In addition, the model contains a prediction for the course of future climate (Fig. 7). Specifically, we take the model output to indicate that orbital forcing will act over the next 23,000 years to continue the general cooling trend that began some 6000 years ago. This effect must be superimposed on variations that will occur at frequencies higher than one cycle per 19,000 years, and on anthropogenic effects such as a possible warming due to an increase in carbon dioxide levels. This conclusion is robust against substantial parametric adjustments (Figs. 4 and 5) and consistent with many (21, 59, 66) but not all (54, 67) earlier predictions.

The past 500,000 years. As noted above, the model's simulation of the isotopic record of ice volume over the past 150,000 years is quite good. But results for earlier times are mixed, and parametric adjustments do little or nothing to improve matters (Figs. 7 and 8). Between 150,000 and 250,000 years ago, most features are reasonably well simulated, and as far back as 350,000 years there are significant correlations. But beyond 350,000 years, the correlation with the geologic record diminishes significantly.

It is useful to analyze two aspects of the model's performance separately. First, we are interested in its ability to simulate the four sharp upward excursions of the isotope record known as terminations I, II, IV, and V (21), which occur at the base of stages 1, 5, 9, and 11, respectively (Fig. 8). Of these, I, II, and IV are well simulated, but V is not. Second, we are interested in the model's ability to simulate the relative magnitude of the main peaks and valleys of the isotope curve. This ability decreases systematically with age, although in some cases (for example, the exaggerated model peak at 170,000 years before present) minor but as yet unresolved discrepancies among published $\delta^{18}O$ curves make it difficult to evaluate the seriousness of model failures. Older instances of model failure occur in isotope stage 8, the upper part of stage 9, the upper part of stage 11, and stage 12. We note that Calder's model does significantly better in stages 8 and 11, but has problems similar to ours in other parts of the older record (Fig. 8).
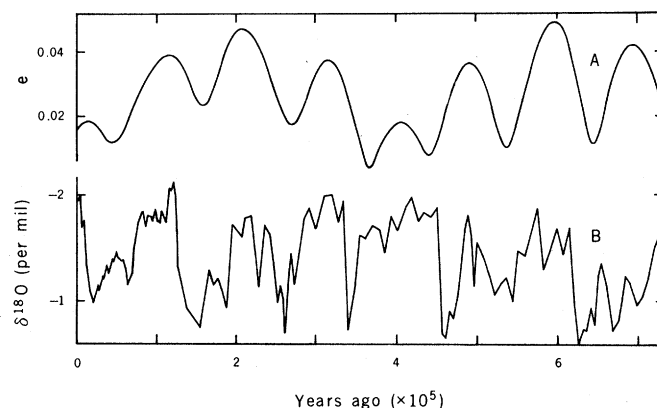
Fig. 10. Eccentricity and global ice volume over the past 730,000 years. (A) Variations in orbital eccentricity calculated by Berger (19). (B) Oxygen isotope curve for deep-sea core V28-238 from the Pacific Ocean. Data from Shackleton and Opdyke (7) are plotted against the PDB standard on the time scale of Kominz et al. (8, 9). Note the phase coherence between the 100,000-year eccentricity cycle and all but the oldest major isotopic fluctuation.

Response spectrum. Another way of evaluating the model's performance is to examine the spectrum of its response. To simplify the discussion, we will refer to the period of spectral peaks in units of K (= 1000 years). As discussed above, the input to our model has periodicities only near 19K, 23K, and 41K, and lacks power at the 100K and 413K eccentricity cycles (Fig. 9A). Yet the isotopic record we are trying to simulate has a dominant periodicity near 100K, in addition to the components near 19K, 23K, and 41K (Fig. 9, C and D). As would be expected from the nonlinearity in our model, the output contains power not only at the forcing periods but also at both periods of the eccentricity cycle (Fig. 9B). Although the resulting spectrum is a better simulation than could be obtained with any linear model, it has too much power at 413K and too little at 100K. Power at 100K has also been found in the models of Weertman (15) and Calder (59). The spectrum of Calder's model (Fig. 9E) contains less 413K power than does the spectrum of our model. However, this is achieved at the expense of introducing spurious power near 200K, which arises as the second harmonic of the 413K cycle when that cycle is clipped by the cutoff in his model. Both models exaggerate the amount of power at 23K and 19K compared with that at 41K.

Improving the Model

The goal of our modeling effort has been to simulate the climatic response to orbital variations over the past 500,000 years (68, 69). The resulting model fails to simulate four important aspects of this record. It fails to produce sufficient 100K power; it produces too much 23K and 19K power; it produces too much 413K

power; and it loses its match with the record around the time of the last 413K eccentricity minimum, when values of *e* were low and the amplitude of the 100K eccentricity cycle was much reduced. All of these failures are related to a fundamental shortcoming in the generation of 100K power. Since the model needs 23K and 19K power to produce its 100K power, there must be a trade-off between the goals of copious 100K power and sparse 23K and 19K power. Moreover, the model cannot distinguish the 413K and 100K eccentricity cycles, so another trade-off takes place here. Finally, a comparison of the warm climatic excursion of 340K to 450K years ago with the eccentricity during that interval (Fig. 10) shows why the model loses its match with the record at that point, and why termination V is not simulated.

A resonance in the climatic system or an intrinsic tendency to oscillate at 100K might resolve all these problems. Unfortunately, the physical basis for such response characteristics seems to be lacking (70).

Another approach to the problem is suggested by comparing the stability diagrams of our model with those of Weertman and Pollard (Fig. 2). Their system functions, when examined at constant input *x*, typically possess two stable fixed points with an unstable point between (71). One stable point is at full glaciation, the other at zero ice. An attractive idea for solving some of the problems cited above would be to use the slow-cooling–rapid-warming mechanism to set up a model that would flip-flop back and forth between stable points in response to changes in the envelope of the precession curve. The stable points would move about and even disappear as *x* varied, thus allowing the high-frequency components of the input to show up in

the fine structure of the output. In addition, a pair of stable points would provide natural upper and lower limits to the output—an appealing feature of the models of Weertman and Pollard.

The existence of an unstable fixed point makes tuning an extremely sensitive task. For example, Weertman notes that changing the value of one parameter by less than 1 percent of its physically allowed range made the difference between a glacial regime and an interglacial regime in one portion of an experimental run, while leaving the rest virtually unchanged (15). Such sensitivity has rendered unsuccessful our preliminary efforts to produce a good system function based on the flip-flop principle. Indeed, it is possible that no function will yield a good simulation of the entire 500,000-year record under consideration here, because nonorbitally forced high-frequency fluctuations may have caused the system to flip or flop in an unpredictable fashion. This would be an example of Lorenz's concept (72) of an almost intransitive system (one whose characteristics over long but finite intervals of time depend strongly on initial conditions).

It is tempting to call upon an unpredictable shift of this kind to explain warm excursions at times when eccentricity was continuously low (the fourth problem mentioned above). However, the regularity of the 100K climatic cycle, and particularly its phase coherence with the 100K eccentricity cycle over the last 650,000 years (Fig. 10), argue for predictability. Thus, there is a basic conflict between the apparent predictability of the record and the sensitivity that models will need in order to reproduce the record accurately. It is therefore very important to decide how many features of the record can be simulated by a deterministic model forced by orbital variations (73). Progress in this direction will indicate what long-term variations need to be explained within the framework of a stochastic model (74), and provide a basis for estimating the degree of unpredictability in climate.

References and Notes

1. J. Croll, *Philos. Mag.* **28**, 121 (1864); *Climate and Time* (Appleton, New York, 1875).
2. M. Milankovitch, in *Handbuch der Klimatologie*, W. Köppen and R. Geiger, Eds. (Borntraeger, Berlin, 1930), vol. 1, part A.
3. _____, R. Serb. Acad. Spec. Publ. 133 (1941) (translated by the Israel Program for Scientific Translations, Jerusalem, 1969).
4. This conclusion is supported by spectral analyses of two paleoclimatic time series derived from deep-sea sediments. One record, from the southern Indian Ocean (5, 6), spans the last 450,000 years. The other, from the equatorial Pacific (7, 8), extends back to the magnetic field reversal that marks the base of the Brunhes Epoch. This stratigraphically important event has recently been dated as 730,000 years ago (9).
5. J. D. Hays, J. Imbrie, N. J. Shackleton, *Science* **194**, 1121 (1976).
6. D. L. Evans and H. J. Freeland, *ibid.* **198**, 528 (1977); J. D. Hays, J. Imbrie, N. J. Shackleton, *ibid.*, p. 529.
7. N. J. Shackleton and N. D. Opdyke, *Quat. Res. (N.Y.)* **3**, 39 (1973).
8. M. A. Kominz, G. R. Heath, T.-L. Ku, N. G. Pisias, *Earth Planet. Sci. Lett.* **45**, 394 (1979).
9. E. A. Mankinen and G. B. Dalrymple, *J. Geophys. Res.* **84**, 615 (1979).
10. C. G. H. Rooth, C. Emiliani, and H. W. Poor [*Earth Planet. Sci. Lett.* **41**, 387 (1978)] assert that power spectrum analysis of the oxygen isotope record cannot be used to search for evidence of astronomical forcing because parts of this record have a steplike character reflecting the rapidity of major deglaciations. Implicit in their argument is the idea that the presence of second- and higher-order harmonics in a Fourier analysis of a signal of this type might introduce sufficient spectral energy to mask orbital influences operating over a frequency range from 1 cycle per 19,000 years to 1 cycle per 41,000 years. But Hays *et al.*, in footnote 66 of (5), examined the same problem in the context of three independent climatic time series (δ^{18}O, T_s, and percentage of *Cycladophora davisiana*) and concluded that the observed spectral peaks cannot be explained as harmonic contaminants. Moreover, they presented evidence for systematic phase relationships with obliquity and precession rather than with the low-frequency components of the record. This rules out the possibility that the observed peaks in climatic spectra could originate in nonsinusoidal low-frequency components. Finally, the observed peaks near frequencies of 1 cycle per 22,000 years and 1 cycle per 41,000 years stand well above any contribution originating in the triangular waves of Rooth *et al.*
11. Kominz and Pisias (12) estimate the percentage of explained variance by integrating cross spectra of squared coherencies between orbital signals (obliquity and precession) and the 730,000-year-long isotopic record of core V28-238.
12. M. A. Kominz and N. G. Pisias, *Science* **204**, 171 (1979).
13. Later in this article, we develop a nonlinear model that can be compared with the geological record. Using techniques explained in (12), N. G. Pisias (personal communication) finds that 34 percent of the isotopic variance over the past 730,000 years in core V28-238 is explained; over the younger parts of this record, the percentage explained is even higher.
14. M. J. Suarez and I. M. Held, *Nature (London)* **263**, 46 (1976); *J. Geophys. Res.* **84**, 4825 (1979).
15. J. Weertman, *Nature (London)* **261**, 17 (1976).
16. D. Pollard, *ibid.* **272**, 233 (1978).
17. S. H. Schneider and S. L. Thompson, *Quat. Res. (N.Y.)* **12**, 188 (1979).
18. A. D. Vernekar, *Meteorol. Monogr. 12* (1972).
19. A. Berger, *Celest. Mech.* **15**, 53 (1977); *Quat. Res. (N.Y.)* **9**, 139 (1978).
20. See G. J. Kukla, *Nature (London)* **253**, 600 (1975), figure 5.
21. W. S. Broecker and J. van Donk, *Rev. Geophys. Space Phys.* **8**, 169 (1970).
22. A. Berger, *Nature (London)* **269**, 44 (1977).
23. See reviews in (3, 18, 19).
24. Calculations in (18) have been widely used. When these curves are compared with those of Berger in (19), the timing of maxima and minima do not differ by more than 1000 years over the past 400,000 years. For older intervals, however, discrepancies between the calculations become significant, and the work of Berger is to be preferred because it includes the effect of more terms. In this article, all calculations involving orbital geometry have been performed on digital data provided by A. Berger, Université Catholique de Louvain, Louvain-la-Neuve, Belgium.
25. L. Pilgrim, *Jahresh. Ver. Vaterl. Naturk. Wuerttemb.* **60** (1904).
26. W. Köppen and A. Wegener, *Die Klimate der Geologischen Vorzeit* (Borntraeger, Berlin, 1924).
27. J. Imbrie and K. P. Imbrie, *Ice Ages: Solving the Mystery* (Enslow, Short Hills, N.J., 1979).
28. Modern calculations of Vernekar (18) and Berger (19) are in fair agreement with those of Milankovitch.
29. For historical reviews, see (5, 21, 27) and J. K. Charlesworth, *The Quaternary Era with Special Reference to Its Glaciation* (Arnold, London, 1957); C. Emiliani and J. Geiss, *Geol. Rundsch.* **46**, 576 (1959); R. F. Flint, *Glacial and Quarternary Geology* (Wiley, New York, 1971); J. M. Mitchell, Jr., in *The Quarternary of the United States*, H. E. Wright, Jr., and D. G. Frey, Eds. (Princeton Univ. Press, Princeton, N.J., 1965), p. 881.
30. M. I. Budyko, *Tellus* **21**, 611 (1969).
31. D. M. Shaw and W. L. Donn, *Science* **162**, 1270 (1968); W. D. Sellers, *J. Appl. Meteorol.* **9**, 960 (1970); B. Saltzman and A. D. Vernekar, *J. Geophys. Res.* **76**, 4195 (1971); A. Berger, *Palaeogeogr. Palaeoclimatol. Palaeoecol.* **21**, 227 (1977).
32. As summarized by the U.S. Committee for the Global Atmospheric Research Program, National Research Council [*Understanding Climatic Change, A Program for Action* (National Academy of Sciences, Washington, D.C., 1975), pp. 136–143], important advances in paleoclimatology have been in quantitative analysis and accurate dating of continuous records in deep-sea piston cores. Major improvements in monitoring include the use of oxygen isotope ratios in microfossil tests [C. Emiliani, *J. Geol.* **63**, 538 (1955)] as an indicator of global ice volume (7, 33) and the use of microfossil assemblages as indicators of water-mass geometry and sea-surface temperature [J. Imbrie and N. G. Kipp, in *The Late Cenozoic Glacial Ages*, K. K. Turekian, Ed. (Yale Univ. Press, New Haven, Conn., 1971), p. 71; R. M. Cline and J. D. Hays, Eds., *Geol. Soc. Am. Mem. 145* (1976)]. Improvements in the time scale have come partly from direct application of radiometric techniques [W. S. Broecker, in *The Quaternary of the United States*, H. E. Wright, Jr., and D. G. Frey, Eds. (Princeton Univ. Press, Princeton, N.J., 1965), p. 737], particularly in marine sediments (21) and uplifted reefs [A. L. Bloom, W. S. Broecker, J. Chappell, R. K. Matthews, K. J. Mesolella, *Quat. Res. (N.Y.)* **4**, 185 (1974)]. But much of the absolute chronology of the sequences under study here is supplied by an indirect method, namely the stratigraphic correlation of specific levels in undated sequences with dated sequences from another location. These correlations, in turn, are based on a framework provided jointly by oxygen isotope stratigraphy [(7, 33); N. J. Shackleton and R. K. Matthews, *Nature (London)* **268**, 618 (1977); C. Emiliani, *Earth Planet. Sci. Lett.* **37**, 349 (1978)], by biostratigraphy [D. B. Ericson and G. Wollin, *Science* **162**, 1227 (1968); J. D. Hays and N. J. Shackleton, *Geology* **4**, 649 (1976); H. R. Thierstein, K. R. Geitzenauer, B. Molfino, N. J. Shackleton, *ibid.* **5**, 400 (1977)], and by paleomagnetic stratigraphy (7, 9).
33. N. J. Shackleton, *Philos. Trans. R. Soc. London Ser. A* **280**, 169 (1977).
34. W. S. Broecker, D. L. Thurber, J. Goddard, T.-L. Ku, R. K. Matthews, K. J. Mesolella, *Science* **159**, 297 (1968).
35. W. S. Broecker, *ibid.* **151**, 299 (1966).
36. R. Fairbanks and R. K. Matthews, *Quat. Res. (N.Y.)* **10**, 181 (1978).
37. Even an excellent correlation between climate and a particular insolation curve $Q(t)$ is no assurance that physical mechanisms operating at the latitude and season represented by $Q(t)$ actually dominate the climatic response. As discussed in the section on model tuning, this interpretative ambiguity exists because a curve nearly identical to $Q(t)$ may be expressed as a linear combination of curves for other latitudes and seasons.
38. W. F. Ruddiman and A. McIntyre, *Geol Soc. Am. Mem. 145* (1976), p. 111.
39. The slowly varying eccentricity coefficient e in the precession effect $e \sin \omega$ results only in a splitting of the 22,000-year spectral peak into a dominant 23,000-year peak and a smaller 19,000-year peak.
40. As discussed below, the problem of explaining the 100,000-year cycle with a simple nonlinear mechanism of the type suggested in (5, 19) and in T. M. L. Wigley [*Nature (London)* **264**, 629 (1976)] hides a second problem. For it is difficult to introduce substantial 100,000-year power into the response without also introducing power reflecting the 413,000-year eccentricity cycle in amounts that are much greater than have been detected in most long climatic records. See Fig. 9D and M. Briskin and W. A. Berggren [*Micropaleontol. Spec. Publ.* **1**, 167 (1975)].
41. N. J. Shackleton and N. D. Opdyke, *Geol. Soc. Am. Mem. 145* (1976), p. 449.
42. G. J. Kukla, *Earth Sci. Rev.* **13**, 307 (1977).
43. K. Hasselmann, *Tellus* **28**, 473 (1976).
44. C. Frankignoul and K. Hasselmann, *ibid.* **29**, 289 (1977); P. Lemke, *ibid.*, p. 385.
45. J. M. Mitchell, Jr., *Quat. Res. (N.Y.)* **6**, 481 (1976).
46. Recent reviews (47–49) show that climate models have been used to investigate the ice-age problem in two distinct ways. One strategy has been to study how a model atmosphere responds to specified changes in its internal forcing fields (ice distribution, ocean temperatures, and so on). This strategy (48–50) has been used in zonally averaged energy-balance models of the

type originated by Budyko (30) and Sellers (51). The same experimental strategy has been used with general circulation models capable of simulating the atmospheric response in three dimensions (52). So far, only the simpler, zonal models have been used in an alternative strategy designed to simulate the climatic response to orbital variations. These experiments are discussed in the following section.

47. S. H. Schneider and R. E. Dickinson, Rev. Geophys. Space Phys. 78, 447 (1974); R. G. Barry, Palaeogeogr. Palaeoclimatol. Palaeoecol. 17, 123 (1975).
48. G. R. North, J. Atmos. Sci. 32, 2033 (1975).
49. R. S. Lindzen and B. Farrell, ibid. 34, 1487 (1977).
50. R. E. Newell, Quat. Res. (N.Y.) 4, 117 (1974); B. Saltzman and A. D. Vernekar, ibid. 5, 307 (1975).
51. W. D. Sellers, J. Appl. Meteorol. 8, 392 (1969).
52. J. Williams, R. G. Barry, W. M. Washington, ibid. 13, 305 (1974); W. L. Gates, J. Atmos. Sci. 33, 1844 (1976); Science 191, 1138 (1976); S. Manabe and D. G. Hahn, J. Geophys. Res. 82, 3889 (1977).
53. In the simplest models, correlations are sought with irradiation curves for a particular latitude and season. Many workers, for example, have followed (3) and chosen summer half-year irradiation at 65°N [C. Emiliani, J. Geol. 74,109 (1966); W. F. Ruddiman and A. McIntyre, Science 204, 173 (1979)]. Others have chosen the same season at 45°N (34, 35) or 50°N (11), or winter half-year irradiation at 55°N [G. J. Kukla, Curr. Anthropol. 9, 37 (1968)]. Another approach has been to use linear combinations of various individual season-latitude curves, including the following curves: summer irradiation at 65°N and 65°S [W. Wundt, Quartär Bibl. (Bonn) 10/11, 15 (1961)], the hemispheric average summer irradiation and the irradiation for summer at 70°N (54), and the annual irradiation at 65°N combined with that for winter between 25°N and 75°N [G. J. Kukla, Boreas 1, 63 (1972)].
54. R. G. Johnson and B. T. McClure, Quat. Res. (N.Y.) 6, 325 (1976).
55. The need for a differential model has been recognized since the time of Milankovitch (3). Although an extensive literature exists on what is called the retardation problem [F. E. Zeuner, The Pleistocene Period (Hutchinson, London, 1959), pp. 200–202; R. M. Fairbridge, Ann. N.Y. Acad. Sci. 95, 542 (1961); W. S. Broecker (35)], only recently has a time-dependent model of the astronomical theory been formulated in terms of differential equations describing the system response.
56. J. Weertman, J. Glaciol. 6, 145 (1964).
57. Weertman (56) used a physical model to estimate that the characteristic growth times of large ice sheets are on the order of 15,000 to 30,000 years. See also J. T. Andrews and M. A. W. Mahaffy, Quat. Res. (N.Y.) 6, 167 (1976).
58. G. E. Birchfield, J. Geophys. Res. 82, 4909 (1977); _____ and J. Weertman, ibid. 83, 4123 (1978).
59. N. Calder, Nature (London) 252, 216 (1974).
60. J. Smagorinsky, in Meteorological Challenges: A History, D. P. McIntyre, Ed. (Information Canada, Ottawa, 1972), p. 29.
61. For most insolation curves the error is less than 1 percent. The exceptions are in high latitudes, where there are seasons of continual darkness or light.
62. Weertman (56) attributes the difference to two effects. First, even if the accumulation rate on a growing ice sheet equals the ablation rate on a shrinking ice sheet, the rate of change in ice volume will be greater on the shrinking sheet than on the growing sheet because the shrinking sheet is more spread out. Second, the accumulation rate is expected to be smaller than the ablation rate.
63. J. Weertman, J. Glaciol. 13, 3 (1974); T. Hughes, G. H. Denton, M. G. Grosswald, Nature (London) 266, 596 (1977); R. H. Thomas and C. R. Bentley, Quat. Res. (N.Y.) 10, 150 (1978); J. T. Andrews, Arct. Alp. Res. 5, 185 (1973).
64. However, there is evidence that ice sheets of modest size, such as those represented by certain substages of isotopic stages 5 and 7, can grow rapidly.
65. Expressed in terms of half-response times, the parameters T_m, T_c, and T_w are 11,800, 29,500, and 7,300 years, respectively.
66. W. S. Broecker, Science 189, 460 (1975); J. M. Mitchell, Jr., "Carbon dioxide and future climate," EDS (Environ. Data Serv.) (March 1977), p. 3.
67. W. Q. Chin and V. Yevjevich, Colo. State Univ. (Fort Collins) Hydrol. Pap. 65 (1974).
68. Although the character of climatic records is fairly constant over the past 600,000 years (7, 38), older Pleistocene records are quite different. For example, isotopic records in the interval from 600,000 to 2 million years ago have much reduced amplitudes and lack the 100,000-year cycle (41). Because the nature of orbital variation is thought to have remained constant over the past 2 million years, we conclude that to understand these long climatic records, it may be necessary to use models whose parameters vary with time (69).
69. V. Y. Sergin, Oregon State Univ. Clim. Res. Inst. Rep. 2 (1978).
70. J. M. Mitchell, Jr. (45), for example, doubts the existence of climatic resonance. But Sergin (69) finds that there is a tendency to oscillate at periods on the order of several tens of thousands of years in a complex model of the climate system. See also E. Källén, C. Crafoord, M. Ghil, J. Atmos. Sci. 66, 2292 (1979).
71. System functions of this kind are discussed in E. Eriksson, Meteorol. Monogr. 8, 68 (1968).
72. E. N. Lorenz, ibid. 8, 1 (1968); Tellus 3, 289 (1969).
73. Other possible deterministic sources of variability will also have to be explored (45). However, since orbital variation is now the only forcing function that can be specified exactly, it is best to exhaust the explanatory power of the astronomical theory first.
74. Building stochastic models to understand the variations unexplained by deterministic models is a relatively undeveloped field for the range of frequencies under consideration in this article (12). A model proposed by Hasselmann (43) generates a red-noise oceanic response to white-noise atmospheric forcing. Almost-intransitive models (72) provide another potentially fruitful avenue of research.
75. Two input parameters, corresponding to the choice of latitude and season (or α and ϕ), are assigned to models that use a single input curve. If the scale of the input is important, then a third parameter is assigned. All other parameters are counted in c_t. For the linear model there is one time constant only; for the nonlinear model there are warming and cooling time constants; for Calder's model there is a ratio of warming and cooling response rates and a critical value of the input; and for Weertman's model there are accumulation and ablation rates, basal shear stress, slope of the snow line, and a critical value of the input.
76. J. Iversen, Dan. Geol. Unders. 5 (1973); J. C. Bernabo and T. Webb. Quat. Res. (N.Y.) 8, 64 (1977); H. E. Wright, Jr., Annu. Rev. Earth Planet. Sci. 5, 123 (1977).
77. N. G. Pisias, Geol. Soc. Am. Mem. 145 (1976), p. 375, table 2.
78. K. J. Mesolella, R. K. Matthews, W. S. Broecker, D. L. Thurber, J. Geol. 77, 250 (1969).
79. N. J. Shackleton, Proc. R. Soc. London. Ser. B 174, 135 (1969).
80. All spectra have been calculated by using standard autocorrelation procedures identical to those described in (5). Let N be the number of sample points, m be the number of lags, Δt be the sampling interval in K years, and C be the constant of a first-difference filter. For the model input and output spectra in Fig. 9, A and B, $N = 501$, $m = 199$, and $\Delta t = 2K$. For the input spectrum in Fig. 9A, $N = 551$, $m = 199$, and $\Delta t = 2K$. In Fig. 9C, $N = 157$, $m = 50$, $\Delta t = 3K$, and $C = 0.998$ for the prewhitened spectrum. In Fig. 9D, $N = 122$, $m = 61$, and $\Delta t = 6K$ for the unprewhitened spectrum and $N = 122$, $m = 47$, $\Delta t = 6K$, and $C = 0.998$ for the prewhitened spectrum. In Fig. 9E, $N = 367$, $m = 133$, and $\Delta t = 3K$. Confidence intervals and bandwidths have been calculated by procedures given in G. M. Jenkins and D. G. Watts [Spectral Analysis and its Applications (Holden-Day, San Francisco, 1968)].
81. Supported by NSF grants OCD75-14934 and ATM77-07755 to Brown University. K. Bryan, I. M. Held, J. M. Mitchell, Jr., T. C. Moore, Jr., W. F. Ruddiman, T. Webb III, and J. Weertman critically read an earlier version of this article and made valuable suggestions for improving it. We thank R. M. Mellor and T. A. Peters for preparing the typescript. This paper will be presented as a Richard Foster Flint lecture at Yale University, New Haven, Conn., on 4 March 1980.

DNA Gyrase and the Supercoiling of DNA

Nicholas R. Cozzarelli

Virtually all duplex DNA exists naturally in a negatively supertwisted form. This supertwisting is an important facet of the processes of DNA replication, transcription, and recombination. Just 4 years ago, a bacterial enzyme that introduces negative supertwists into DNA was discovered by Gellert et al., who christened it DNA gyrase (1). This article describes how the rapidly advancing studies of gyrase have traversed a spectrum of topics of contemporary interest including the mechanism of supercoiling, the energetics of macromolecular movement, the conversion of DNA into complex topological forms, the site-specific binding of enzymes to DNA, the reversible association of enzyme subunits, and the mechanism of inhibitors of DNA synthesis. It is a propitious time for a review of gyrase, since critical features of the enzyme can now be explained satisfactorily by the recently proposed mechanism termed sign inversion (2). This article focuses on the enzyme from Escherichia coli about which most is known (3).

The author is a professor of biochemistry at the University of Chicago, 920 East 58 Street, Chicago, Illinois 60637.

953